Horizontal trajectory based mobile multi-sink routing in underwater sensor networks

Vijayalaxmi R. Patil[1], Anita Kanavalli[2]
[1]Department of Information Science and Engineering, Dr. Ambedkar Institute of Technology, Bangalore, India
[2]Department of Computer Science and Engineering, Ramaiah Institute of Technology, Bangalore, India

Article Info

ABSTRACT

Scientific, commercial, exploration, and monitoring applications of underwater sensor networks have drawn the attention of researchers toward the investigation of routing protocols that are robust, scalable, and energy efficient. This has brought significant research in network layer routing protocols. Irrespective of the field of application it is desirable to increase network lifetime by reducing energy consumed by sensor nodes in the network or by balancing energy in the entire network. Energy balancing refers to the uniform distribution of the network's residual energy such that all nodes remain alive for a long time. It requires uniform energy consumption by each sensor node in the network instead of the same node being involved in every transmission. In this paper, we discuss two routing methods for three-dimensional environments in which the water region under monitor is divided into subregions of equal height and each subregion has a sink. Nodes in the subregion send data to the sink designated for that subregion. The first method called static multi-sink routing uses static sinks and the second method called horizontal trajectory-based mobile multi-sink routing (HT-MMR) uses mobile sinks with a horizontal trajectory. Simulation results show that the proposed HT-MMR reduces average energy consumption and average energy tax by 16.69% and 16.44% respectively. HT-MMR is energy efficient as it enhances network lifetime by 11.11%.

Corresponding Author:

Vijayalaxmi R. Patil
Department of Information Science and Engineering, Dr. Ambedkar Institute of Technology
Bangalore, India
Email: vijumalghan@gmail.com

1. INTRODUCTION

Approximately 70% of the earth's surface is covered by water. Underwater sensor networks (UWSNs) find a wide range of applications in diverse fields. Observations of temperature, pressure, humidity, and salinity are some of the scientific applications of UWSNs. Exploration applications include the exploration of natural resources like oil, minerals, and gas. UWSNs may be utilized for monitoring plastic debris, acidification, and toxins for pollution control of the aquatic environment. Marine life monitoring, fish farming, aquatic plants, and coral reef monitoring are some examples of habitat monitoring applications. UWSNs may be used for detecting and preventing natural disasters like floods, oil spills, tsunamis, volcanic eruptions, and seaquakes. Military applications include surveillance, enemy movement detection, port, and harbor monitoring. UWSNs are helpful in providing assistance during navigation by detecting objects. Cable monitoring and pipeline monitoring for leakage or oil spill are also some more monitoring applications of UWSNs. UWSNs differ in many aspects when compared with terrestrial wireless sensor networks (TWSNs). Table 1 gives the comparison of TWSNs and UWSNs with respect to various parameters.

Table 1. TWSN and UWSN comparison

Parameter	TWSNs	UWSNs	Parameter	TWSNs	UWSNs
Deployment region	Land	Underwater	Latency	Less	More
Physical medium	Air	Water	Node mobility	Less	High
Signal for communication	Radio	Acoustic	Network	2D	1D, 2D, 3D, 4D
Speed of propagation	3×10^8 m/s	1500 m/s	Bandwadth	High	Low
Error probability	Low	High	Sensor size	Small	Large
Propagation delay	Low	High	Sensor cost	Low cost	Expensive

Underwater routing protocols may be classified as vector-based, depth-based, cluster-based, opportunistic, and intelligence-based under water routing protocols (UWRPs). All vector-based routing protocols [1]–[5] are location-based protocols which means that each node is aware of its location in the network. Table 2 gives the list of abbreviations and expansions of various protocols discussed in this section. Xie et al. [1] proposed a vector-based forwarding (VBF) protocol in which a single vector pipe of length equal to the distance between the source and destination is used. Because of the fixed length and fixed orientation of the virtual pipe, there exists a void problem and also nodes within the pipe die faster. Nicolaou et al. [2] improved the robustness of the routing protocol by altering the routing pipe length instead of keeping it fixed to the distance between the source and destination. In hop-by-hop vector-based forwarding (HH-VBF) the orientation of the vector pipe is dynamic for every hop. This reduces the death rate of nodes lying inside the virtual pipe. Pouryazdanpanah et al. [3] used two sinks to improve the packet delivery ratio in dual sink vector-based forwarding (DS-VBF). Zhang et al. [4] focused on link reliability in reliable hop-by-hop vector-based forwarding (RHH-VBF). Wu and Sun [5] proposed reliable energy-efficient vector-based forwarding (REEVBF) which is both a reliable and energy-efficient routing protocol. The reliability of data transmission is improved by adopting a routing confirmation mechanism.

Table 2. UWSN routing protocol abbreviations and expansions

Abbreviation	Protocol Expansion	Abbreviation	Protocol Expansion
VBF	Vector based forwarding	IHENPC	Improved high-energy node priority clustering
HH-VBF	Hop by hop vector-based forwarding	EERCA	Energy efficient routing for UWSNs-A clustering approach
DS-VBF	Dual sink vector-based forwarding	EnOR	Energy aware opportunistic routing
RHH-VBF	Reliable hop by hop vector-based forwarding	EBOR	Evidence theory based opportunistic routing
REEVBF	Reliable energy efficient vector-based forwarding	EECOR	Energy-efficient cooperative opportunistic routing protocol
DBR	Depth based routing		
EEDBR	Energy-efficient depth-based routing	QDTR	Machine learning based routing protocol for underwater delay tolerant networks
SMDBR	Sink mobility in depth-based routing	REBAR	Reliable and energy balanced routing algorithm for UWSNs
CDBR	Forwarding nodes constraint-based depth-based routing	DDD	Delay-tolerant data Dolphin
LCDBR	Link state and forwarding nodes constraint-based depth-based routing	E-PULRP	Energy optimized path unaware layered routing protocol
SEEC	Sparsity-aware energy efficient clustering	REEP	Reliable and energy efficient routing protocol
CSEEC	Circular sparsity-aware energy efficient clustering	L2-ABF	Layer by layer angle-based flooding
CDSEEC	Circular depth-based sparsity-aware energy efficient clustering	BEER	Balanced energy efficient rectangular routing protocol
HENPC	High-Energy node priority clustering	EVA-DBR	Energy-efficient and void avoidance depth-based routing

Depth-based UWRPs [6]–[10] are location-free protocols that utilize depth information of nodes during the next-forwarding node selection. The depth of the node from the water surface is the key attribute considered for the selection of the next-forwarding node. The nodes which are at a lower depth compared to the source node depth become members of the candidate set of forwarding nodes. The selection of the actual forwarding node from the candidate set depends on other factors like residual energy, depth threshold, and signal-to-noise ratio (SNR) of the sensor node. DBR is the most popular routing protocol proposed by Yan et al. [6] and it uses multi-sink architecture. Wahid et al. [7] proposed energy efficient depth based routing (EEDBR) where both depth and residual energy information are considered for choosing the next forwarding node, to improve network lifetime. Ilyas et al. [8] used a mobile sink with an elliptic path for gathering data and depth information for choosing the next-forwarding node in sink mobility in depth-based routing (SMDBR), to improve network lifetime and energy consumption. Mahmood et al. [9] restricted the number of neighbor nodes receiving data, to improve energy efficiency in the constraint based DBR (CDBR) protocol. The neighbor nodes at a depth less than the sender node depth are considered and among these

nodes, only the nodes having higher depth threshold were selected as next-forwarding nodes. In CDBR data is forwarded to all members of the next forwarding set. To further save energy, Kaur and Goyal [10] proposed the selection of a single optimal next-forwarding node in link state and forwarding nodes constraint-based depth-based routing (LCDBR). Hence sender node sends data to the node which is at minimum depth towards the sink.

Cluster-based UWRPs [11]–[14] involved cluster formation as an initial step, followed by a selection of cluster heads (CH). CH receives data from respective cluster members (CMs) and received data is aggregated by CH and then sent to another cluster's CH. The process is continued until the sink receives data. Sher *et al.* [11] proposed sparsity-aware energy efficient clustering (SEEC), circular sparsity-aware energy efficient clustering (CSEEC), and CDSEEC protocols which differ in network architecture. SEEC divides network area into logical regions; CSEEC divides the area into concentric circles, which in turn are divided equally. The network area is divided into two semicircles in CDSEEC. The semicircle at the bottom is further divided into concentric semicircles. Sinks used in networks are static and mobile in nature. CH selection is based on the depth and residual energy of the node. Both SEEC and CSEEC employ multi-hop or single-hop routes for the transmission of data. If the sink is not within CH's transmission range, a multi-hop route is used; otherwise, a single-hop route is used. Data transmission in CDSEEC differs from data transmission in SEEC and CSEEC. CDSEEC considers the depth of the node while selecting the next-forwarding node. High-energy node priority clustering (HENPC) which is MI-based UWSNs was proposed by Wang *et al.* [12]. The hexagonal nature of clusters ensures that the numbers of members in clusters are equal. Every round of CH is updated based on fixed radius and CM residual energy. AUV is used for collecting data from CH. Improved high-energy node priority clustering (IHENPC) was proposed by Wang *et al.* [13] to address the energy hole problem of HENPC. In IHENPC, CH updates every round based on residual energy and distance of CMs. The jellyfish breathing process is followed for cluster formation and based on node density, cluster size changes dynamically. The optimal cluster is determined by the Voronoi diagram. Khan *et al.* [14] presented energy efficient routing for UWSNs-a clustering approach (EERU-CA) for routing in UWSNs. EERU-CA uses special nodes having high energy and transmission power. Special nodes are deployed at different depths and locations underwater. Special nodes closest to the sink can transfer data directly to it. All other special nodes acting as CH involve in data collection and aggregation. The aggregated data is sent to special nodes closer to the sink. The energy and distance of special nodes are criteria for selecting special nodes for forwarding data. The special node having maximum energy and minimum distance toward the sink is chosen to save energy.

In opportunistic UWRPs [15]–[17], the node nearest to the destination node is chosen for data forwarding. It uses the broadcasting nature of UWSNs. Coutinho *et al.* [15] proposed EnOR where the forwarding candidate nodes transmission-priority level is rotated by taking link-reliability, residual energy, and packet advancement to enhance network lifetime. EBOR protocol proposed by Jin *et al.* [16] determines the optimal next hop by considering packet delivery probability and residual energy as evidence. The participating forwarding neighbor-nodes count is reduced on the computation of trust, which in turn reduces energy consumption. Source node schedules packet transmission based on the node's trust value. It balances energy in the network and thereby enhances network lifetime. Rahman *et al.* [17] proposed an EECOR protocol in which the forwarding-relay-set is determined by the source node based on depth and network topology information. In fuzzy logic-based relay selection, every relay node's Packet delivery probability and energy consumption ratio are used to choose the best relay node from the relay set. The forwarding relay node's holding timer is designed to schedule packet transmission so as to prevent packet collisions and retransmissions.

Intelligence-based UWRPs [18]–[20] used machine learning, reinforced learning (RL), or deep-learning algorithms for the selection of the next forwarding node. Hu and Fei [18] proposed a machine-learning-based adaptive routing named QELAR, which employs reinforced learning. Q-learning technique is used, and Q-value is computed for each successful packet transmission. The agent's performance in Q-learning depends on the value of the reward which is based on the agent's action. Formulation of the reward function in QELAR is done using energy distribution and the node's residual energy. QELAR has achieved an enhanced network lifetime. Hu and Fei [19] proposed machine learning based routing protocol for underwater delay tolerant networks (QDTR) based on RL using the Q-learning technique. The reward function is formulated by considering sink distance to node, residual energy of node, and density of neighboring node. QDTR improves the delivery ratio with less energy. Wang and Shin [20] calculated Q-value on the basis of remaining energy and transmission delay in Q-learning based energy-delay routing (QL-EDR). The Q-learning algorithm computes rewards based on regulatory-factor to balance transmission delay and energy consumption. Chen *et al.* [21] addressed reliability, energy efficiency, and void problem in reliable and energy balanced routing protocol (REBAR). Magistretti *et al.* [22] focused on energy-saving issues in delay-insensitive networks in delay-tolerant data Dolphin (DDD) protocol. Sensors exploit one-hop

communication with dolphins. Gopi *et al.* [23] used a concentric sphere layering structure. Based on minimum overall energy and probability of successful packet transmission, the radii of spheres and the node's transmission energy in each layer are chosen. Rahman *et al.* [24] proposed reliable, scalable, self-organizing, and energy efficient reliable and energy efficient routing protocol (REEP). The time of arrival (TOA) concept is adopted for calculating the distance to sink. The forwarding path is established based on sink distance and residual energy information. Ali *et al.* [25] addressed the node swaying issue and node energy consumption in the L2-ABF protocol. Angle base flooding approach increases reliability and to save power, flooding cone length, and power level are adjusted. Abbasi *et al.* [26] addressed energy balancing and energy efficiency problems in the balanced energy efficient rectangular routing (BEER) protocol. Through the mobility of the sink, the maximum network area is covered, network lifetime and throughput are enhanced, and the energy consumption is reduced. Ghoreyshi *et al.* [27] addressed the void problem in the proposed energy-efficient and void avoidance depth based routing (EVA-DBR) protocol.

       Node mobility caused due to water currents, high error probability, low bandwidth, high delay, and limited battery power are challenges of UWSNs. In this paper, the authors have discussed two methods of routing in UWSNs viz static multi-sink routing (SMR), and horizontal trajectory-based mobile multi-sink routing (HT-MMR). The mathematical models are formulated, and routing algorithms are devised for each method. The routing methods are simulated using the NS-2.35 simulator. The performance evaluation of each routing method is carried out by calculating energy consumption, energy tax, throughput, and the number of live nodes. The performance metrics obtained are compared and analyzed. To estimate the true population, means of energy consumption, energy tax, and throughput, confidence intervals are calculated and tabulated. The following assumptions are made for the work carried out: i) UWSN is three-dimensional (3D); ii) all UW-sensors are static and deployed layer-wise; iii) each layer has a sink; iv) all sensors including the sink have the same initial energy; v) sink in SMR is static and sink in HT-MMR is mobile with horizontal trajectory; vi) mobile sinks in HT-MMR move with constant speed; and vii) if data from source node reaches the sink designated for the layer it is assumed that data is delivered.

2. RESEARCH METHOD
2.1. Problem definition
       In water monitoring applications of UWSNs as illustrated in Figure 1, sensors are deployed both on the surface and below the water surface. Underwater (UW) sensors sense data and send information to the sink. The sink in turn will send data to the onshore base station (BS). From on-shore BS via satellite communication data is sent to off-shore BS for further data processing and analysis. UW sensors have limited energy sources i.e., battery life. Hence energy of sensors has to be used more efficiently. In the existing system sensor nodes send data to the sink by forwarding data to a node in a path from source to sink in a hop-by-hop fashion. Sensor energy is consumed both during the transmission and also the reception of data. Due to the involvement of more nodes in the path between the source and sink energy consumption of the network is increased. We propose an energy-efficient routing method where mobility is introduced to the sink for reducing the number of hops required to transmit data to the sink and thereby energy consumption of sensors is reduced, and the lifetime of sensors is increased. In existing, routing methods sensors are deployed randomly, and sinks are generally deployed on water surfaces. Many routing methods employing layered multi-sink architecture are also available in the literature. In existing methods, data may be sent to any one of the sinks, but the proposed method differs in providing a sink to each layer, and data is sent to the sink designated for that layer. This technique helps in the uniform distribution of load on every sink.
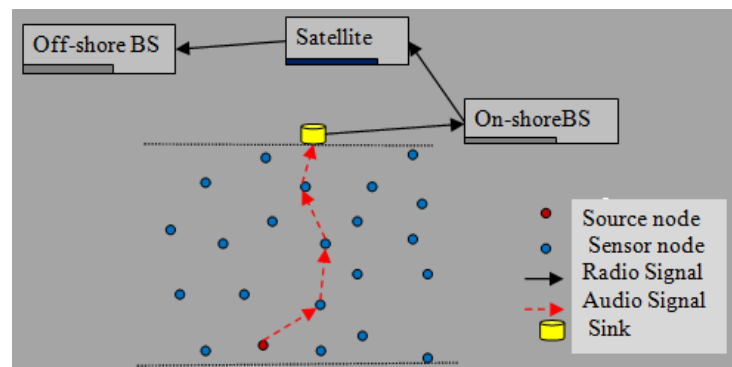

Figure 1. Underwater application scenario

2.2. Mathematical model of proposed method

This section discusses mathematical models of SMR and HT-MMR routing methods. Let the length, breadth, and height of the water region under monitor be denoted as *L, B,* and *H,* respectively. The region is divided into sub-regions of equal sizes. The surface of the sub-region which extends from the top surface to depth D forms Layer-1 (L1). The surface of the subregion which extends from depth D to 2D from the water's top surface forms Layer-2 (L2). Similarly, Layer-3 (L3) is the surface of the water sub-region extending from depth 2D to 3D, and Layer-4 (L4) is the surface of the water subregion extending from depth 3D to 4D. The same number of sensors is deployed on each of the layers and each layer has one sink. *M1, M2, M3,* and *M4* denote sinks deployed on *L1, L2, L3,* and *L4,* respectively. Sinks are stationary in the SMR method. But each sink is assumed to have a horizontal trajectory at a predefined speed in the HT-MMR method. Each horizontal trajectory includes sink movement from the right-to-left end and from the left end back to the right end of the layer of water. Always sensed data is forwarded to a sink which is deployed on the layer where sensors are also deployed. Each sink speed is set to the specified value and is assumed that all sinks move with the same constant speed from right to left direction and then from the left-to-right direction. During this time if sensors have data to send, they send data to the sink. All sensor nodes except sinks are assumed to be stationary.

Let N denote the total number of layers in the region of dimension *LXBXH.* Interlayer distance D is given by (1).

$$D = \frac{H}{N} \ where \ H \ is \ height \ of \ region \ and \ N \ is \ number \ of \ layers \tag{1}$$

Li represents Layer-*i* where $i \in \{1, 2, ..., N\}$. Mathematically UW sensor 3D deployment position on *Li* is expressed as *P(x,y,z)* where *0≤x≤L* and *0≤y≤* B and *z* is given by (2).

$$z = H - (i - 1) * D \ where \ i \ represents \ Layer \ number \ and \ D \ is \ inter \ layer \ distance \tag{2}$$

The deployment position of Layer-i sink in 3-dimension space is mathematically expressed as P(*x,y,z*) where *x=L; y=B/2* and *z=H-(i-1)*D* where i represents Layer number and D is interlayer distance.

The instantaneous position of Layer-*i* mobile sink having speed *MSk* and horizontal trajectory from right to left is mathematically given by (3) to (5),

$$x(t) = x - MSk * t \ where \ t \ is \ time \ in \ Sec \ ; \ t \geq 0 \tag{3}$$

$$y(t) = \frac{B}{2} \ ; t \geq 0 \tag{4}$$

$$z(t) = H - (i - 1) * D; \ t \geq 0 \tag{5}$$

where *i* is layer number and *D* is interlayer distance. Let mobile sinks reach the left end of the region at time t=T_L. On reaching the left end horizontal trajectory of the Layer-i sink's instantaneous position is defined by (6) to (8),

$$x(t) = x + MSk * (t - 2 * TL) \ where \ t \ is \ time \ in \ Sec; t \geq TL \tag{6}$$

$$y(t) = \frac{B}{2} \ ; \ t \geq TL \tag{7}$$

$$z(t) = H - (i - 1) * D; \ t \geq TL \tag{8}$$

where *i* is layer number and *D* is interlayer distance.

2.3. Routing methods

In this section, we discuss two routing methods *viz.* SMR [28] and proposed HT-MMR. The sensors may be deployed in 3D or two-dimensional (2D) environments. In a 2D environment, sensors are deployed on the water surface, whereas, in a 3D environment, sensors are deployed at various depths. Hence deployment position of sensors in the 2D environment is represented as *P(x, y)*, and in the 3D environment sensor position is represented as *P(x, y, z)* where *z* represents the depth of the sensor from the water surface. For sensors deployed on the water surface *z* is zero and for the sensors deployed on a waterbed, *z* is the depth of the waterbed from the water surface. In the presented work sensors are deployed in the 3D environment.

2.3.1. SMR method

In this method all sinks are static. They collect data packets sent from UW sensors. SMR works in two phases: the network initialization phase and the data transmission phase. During the network initialization phase sensors are deployed layer-wise and for each layer, a UW-sink is deployed. All UW sensor nodes and UW sinks are assumed to be stationary and configured with the same initial energy. During the data transmission phase packet is sent to the sink either by single hop or by multi-hop based on the sender and sink position. If the sink is within transmission range of the sender, the packet is directly sent to the sink otherwise sent to the sink by multi-hop transmission. Figure 2 illustrates static multi-sink architecture. UW sensor communication uses audio signals. UW sinks are equipped with both audio and radio modems. Hence, sensor-to-sink communication is through audio.
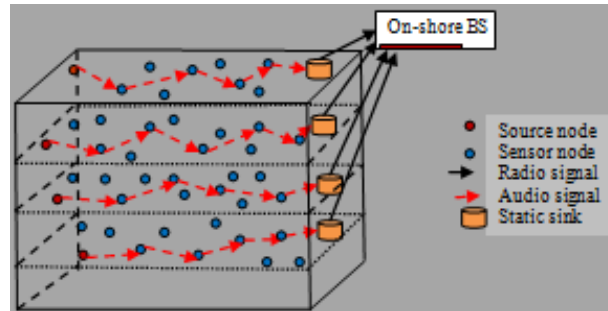

Figure 2. Network model of SMR

2.3.2. HT-MMR method

In this proposed method all sinks are mobile and have horizontal trajectories. HT-MMR works in 3 phases: i) network initialization phase, ii) sink mobility phase, and iii) data transmission phase. The network initialization phase is the same as the SMR method. During the sink mobility phase, the horizontal trajectory is set to sink, and the sink moves with the predefined speed in right to left direction. On reaching the predefined end of the deployment region sink moves in the left-to-right direction. During the data transmission phase source sends the packet to the sink either by single hop or by multi-hop based on the mobile sink position. If the mobile sink is within transmission range of the sender, the packet is directly sent to the sink otherwise sent to the sink by multi-hop transmission. SMR works in 2 phases and HT-MMR works in 3 phases. HT-MMR is basically similar to SMR except for the sink mobility phase. It is this phase that contributes to improvements in performance. Figure 3 illustrates network architecture and mobile sinks which have horizontal trajectories. HT-MMR architecture differs from SMR architecture in sink mobility and its trajectory.
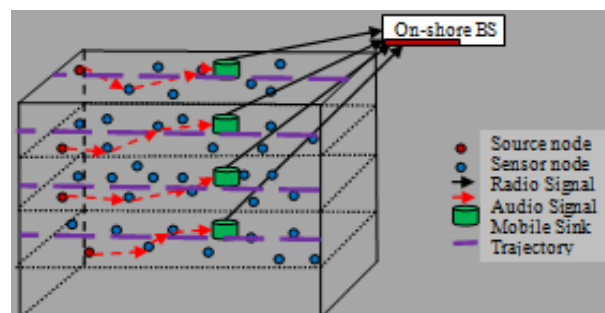

Figure 3. Network model of HT-MMR

2.3.3. Algorithms of SMR and HT-MMR routing methods

The pseudo-codes for the routing mechanism and data transmission are given in Figure 4. In this algorithm $L1, L2 ... LN$, represent layers where N represents the total number of layers in network architecture. MSk represents sink speed. For the static sink, MSk has to be set to zero. All layers are deployed with the same number of homogeneous sensor nodes meaning that they have the same initial energy. S_{11},

$S_{12,}... S_{1M}$, represent M sensors on layer-1 and *M1* is the sink designated for layer-1. Similarly, $S_{21}, S_{22}... S_{2M}$ are *M* sensors on layer-2 and *M2* is the sink designated for layer-2. In general, $S_{i1}, S_{i2,} S_{iM}$ are sensors deployed on layer *Li* where *M* is the count of sensors on layer *Li* and $M_1, M_2 ... M_N$ are static sinks designated for layers *L1, L2... LN* respectively. *Sij* in the algorithm denotes a sensor that has sensed data and has a packet to send. The first subscript *i* represents that it is a sensor belonging to layer-i and the second subscript *j* represents the sensor number. As each layer has a total of *M* sensors *j* may take any value in the range *1... M*.

The pseudo-code algorithm for the routing mechanism and data transmission for HT-MMR are given in Figure 5. In this algorithm, *L1, L2, ..., LN* represent layers where *N* represents total layers in network architecture; *Si1, Si2, ..., SiM* are sensors deployed on layer *Li* where *M* is the count of sensors on Layer *Li*; $M_1, M_2 ....M_N$ represent Mobile sinks designated for *L1, L2, ..., LN* respectively; *MSk* represents Mobile-Sink speed. All mobile sinks are set to move with the same speed and trajectory. Once the trajectory is set, simultaneously all mobile sinks start moving with constant speed along the set trajectory. *Sij* in the algorithm denotes a sensor that has sensed data and has a packet to send. The first subscript *i* represents that it is a sensor belonging to layer-i and the second subscript *j* represents the sensor number. As each layer has a total of *M* sensors *j* may take any value in the range *1.... M*.

```
Input:    N: Number of Layers (Sinks)
MSk:  Sink Speed
Step 1: For each Layer Li, i←1, 2....N
            Set sink speed MSk=0; //Sink is set to be static
        // Data Transmission
Step2: If(Sensor Sij of Li has  packet to send) then
Step3: If(Mi is within transmission range of Sij)then
            // Single-hop transmission
Step4:  Sij forwards packet directly tosinkMi
            Else
        //Multi-hop transmission
Step5:  Sij forwards packet to Mi via intermediate
            nodes
End if
End if
Step 6: Repeat steps 2 to step5 for specified time

Step7: Return
```

Figure 4. Routing algorithm for SMR

```
Input:N: Number of Layers ( Mobile Sinks)
MSk:   Mobile Sink Speed
Step 1: For  each Layer Li , i ←1,2....N
            Set Mobile sink speed toMSk;
Step 2:  Trajectory ←Right_to_Left
Step 3: For each mobile sink Mi ←1,2....N
            Sink_trajectory← Trajectory ;
Step 4: While (Sink Mi  not reached other end )
        // Data Transmission
Step 5: If ( Sensor  Sij of Li  has data packet to send)  then
Step 6: If ( Mi is within transmission range of  Sij ) then
        // Single-hop transmission
Step 7: Sij forwards packet  directly to Mi
            Else
        //Multi-hop transmission
Step 8: Sij forwards packet to Mi via intermediate nodes
            End if
        End if
    End While
Step 9: Trajectory ←Left_to_Right
Step 10: Repeat  steps  4 to step 8 for specified time
Step 11: Return
```

Figure 5. Routing algorithm for HT-MMR

The complexity of SMR and HT-MMR algorithms may be analyzed as stated below. With the assumption that at least one node is available for forwarding in the transmission range, the best case occurs when the forwarding node is situated at the outline of the transmission range in the direction towards the sink position due to a minimum number of hops. The worst case occurs when no forwarding node lies within the transmission range leading to a void problem. The average case occurs when the source successfully delivers data to sink with a number of hops more than the minimum number of hops. In the case of HT-MMR best case occurs when the mobile sink is within the transmission range of the sender as there is a single hop transmission. The worst case occurs when the mobile sink is at the farthest end (successful delivery of data) or there are no forwarding nodes in the transmission range leading to a void problem similar to SMR. The average case occurs when the source delivers data to the sink in 2, 3, and 4 hops depending on the vicinity of the mobile sink.

2.4. Experimental setup

The simulation tool used for the experiment is NS-2.35 an event-driven network simulator. For the performance evaluation of the proposed HT-MMR method against the SMR method, both methods need to be simulated in identical network environments. Hence network dimension, energy model of sensors, and other simulation parameters used for both methods must be kept the same. The simulations of both SMR and HT-MMR protocols were conducted using the same simulation parameters and network setup. The performance is evaluated in terms of performance metrics average energy consumption, energy tax, throughput, and a number of live nodes. HT-MMR and SMR results are then compared and analyzed.

In the experimental setup, sensors are deployed in a region of 1 km^3 with an interlayer distance of 250 m. Each layer has in all 5 nodes and among them, one node will act as a sink. All nodes including sinks are stationary in the SMR method, but in the HT-MMR method, sinks are configured to have mobility with a horizontal trajectory. Each node including sink nodes has initial energy of 50 Joules. Energy consumed for transmission and reception of data are set to 2 and 0.1 Watts, respectively. Idle and sleep power assigned for each node is 1 and 0.1 mW, respectively. The size of the data packet used is 1 KB. The transmission range used for simulation is 100 m. Results are obtained with the SMR method by keeping all sink speeds equal to zero. HT-MMR simulation is carried out for two different mobile sink speeds 50 m/sec and 100 m/sec. During simulation mobile sink horizontal trajectory is set from one end of the layer to the other end of the layer and also back to the original position. Simulations are carried out layer-wise separately for 5, 10, 15, and 20 nodes. Simulation parameters and their values are summarized in Table 3.

Table 3. Parameter description

Parameter	Value	Parameter	Value	Parameter	Value	Parameter	Value
Dimension	3D	Sinks per layer	1	Power for reception	0.1 W	Transmission Range	100 m
Terrain	1 Km^3	Initial energy	50 J	Sleep Power	0.1 mW	Packet size	1 KB
Inter layer distance	250 m	Power for transmission	2 W	Idle Power	1 mW	Traffic	CBR

In the first experimental setup nodes, 0-4 are deployed on the water surface as layer-1 nodes as illustrated in Figure 6. Node 4 is a mobile sink that moves in a horizontal trajectory. The simulation was carried out with nodes deployed only on layer-1. Simulation results illustrate the different positions occupied by sinks with the advancement of time. The mobile sink moves at a speed of 100 m/sec from right to left and then from left to right with the same constant speed. The data is transmitted in single-hop or multi-hops to the mobile sink as illustrated in Figure 6. In the second experimental setup, nodes are deployed on 2 layers. Nodes 0-4 are deployed on layer-1 and nodes 5-9 are deployed on layer-2. Nodes 4 and 9 are mobile sinks of layer-1 and layer-2, respectively. Both mobile sinks move in a horizontal trajectory with a constant speed of 100 m/sec as illustrated in Figure 7. Simulation results illustrate the different positions occupied by mobile sinks with the advancement of time. The data is transmitted in single-hop or multi-hops to respective mobile sinks.

In the third experimental setup, nodes are deployed on 3 layers. Nodes 0-4, nodes 5-9, and nodes 10-14 are layer-1, layer-2, and layer-3 nodes, respectively. Nodes 4, 9, and 14 are mobile sinks of layer-1, layer-2, and layer-3, respectively. All mobile sinks move in a horizontal trajectory with a constant speed of 100 m/sec as illustrated in Figure 8. Simulation results illustrate the different positions occupied by mobile sinks with the advancement of time to collect data from UW sensors. The data is transmitted in single-hop or multi-hop to respective mobile sinks. In the last experimental setup, nodes are deployed on 4 layers. Nodes 15-19 are added to the previous setup as layer-4 nodes. Node 19 is the mobile sink. The simulation was carried out for 20 sec and the results obtained are illustrated in Figure 9. The above procedure was repeated by setting the mobile sink speed to 50 m/sec.
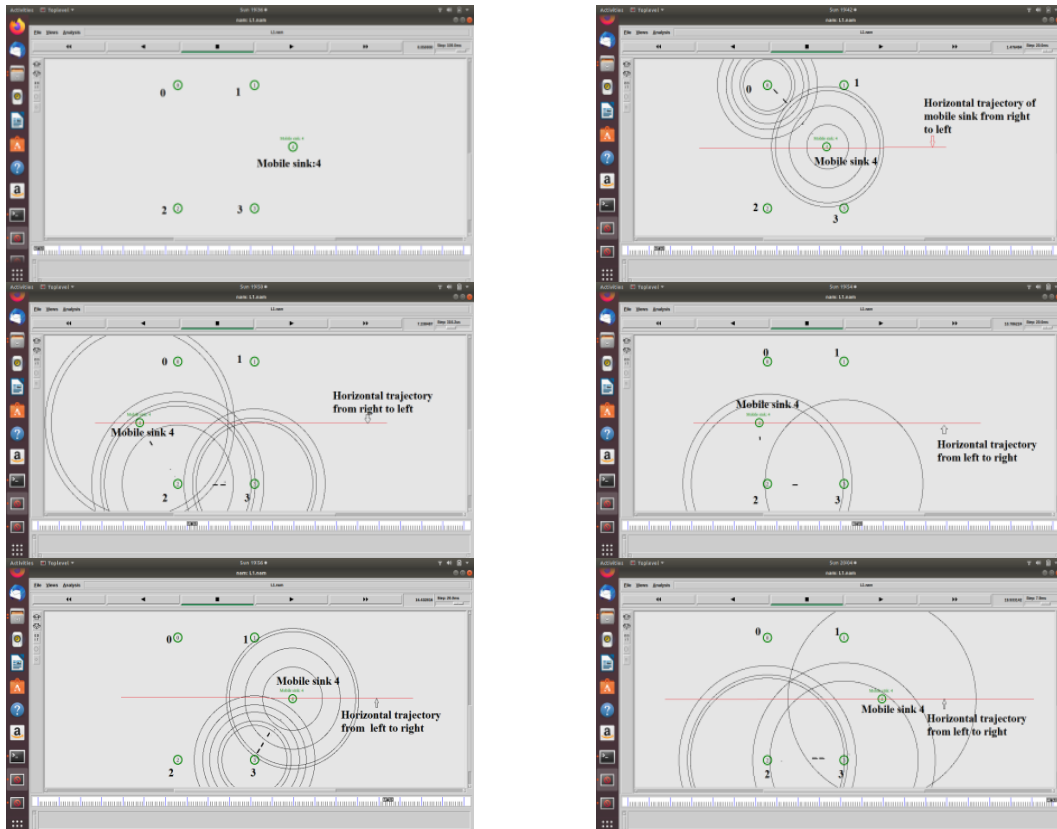
Figure 6. Simulation results with 5 nodes (HT-MMR)
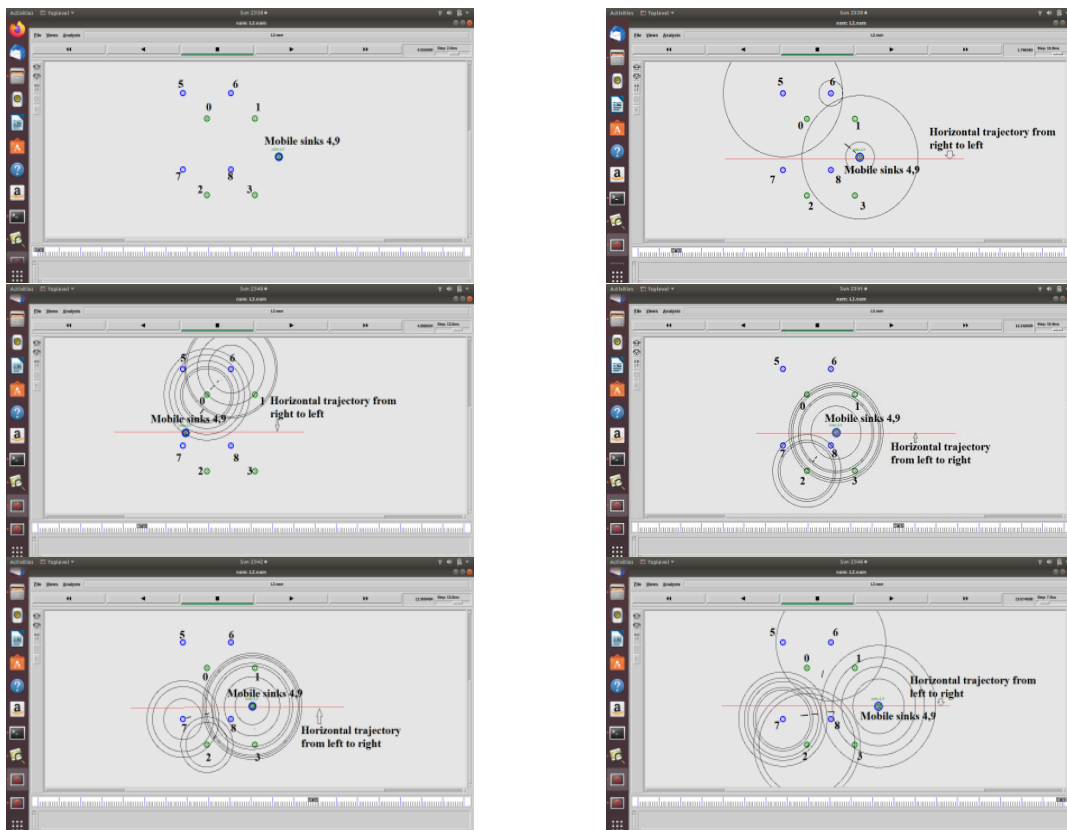

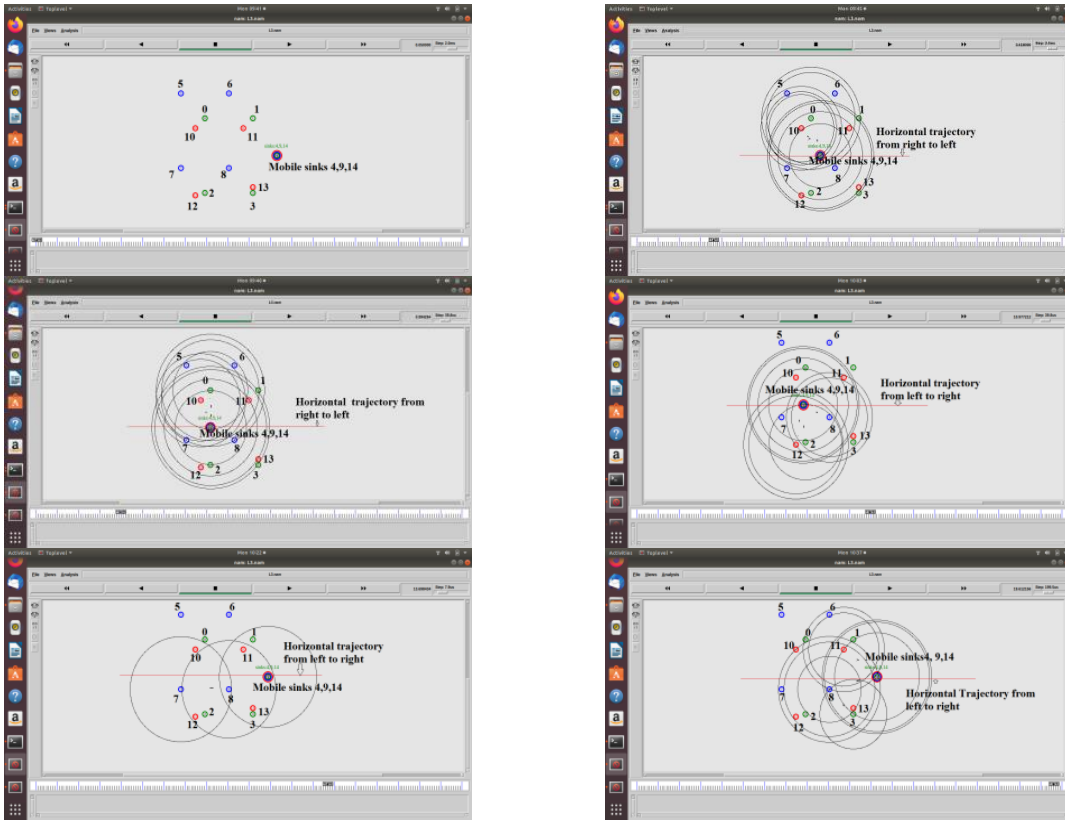Figure 7. Simulation results with 10 nodes (HT-MMR)

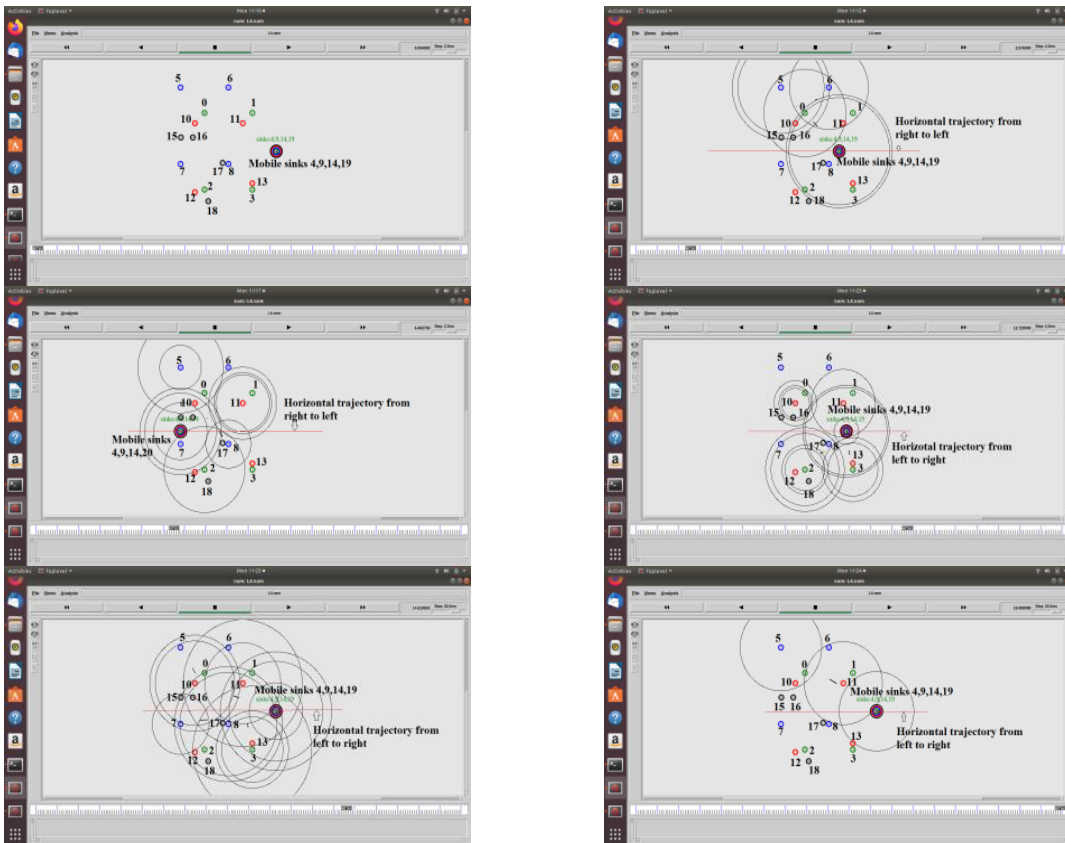Figure 8. Simulation results with 15 nodes (HT-MMR)

Figure 9. Simulation results with 20 nodes (HT-MMR)

3. RESULTS AND DISCUSSION

Average energy consumption (AEC), energy tax (ET), throughput, and a number of live nodes are chosen for the routing protocol performance study. For an energy-efficient routing protocol AEC, ET must be low, and a number of live nodes must be high. Throughput must be high for a given routing protocol. Table 4 gives the summary of calculated values of AEC, ET, throughput, and live nodes for different network sizes.

Table 4. Numerical values of simulation results

Average Energy Consumption in Joules				Energy Tax in mjoules per Packet				Throughput in Bits per sec			
Nodes	SMR	HT-MMR: 50 m/sec	HT-MMR: 100 m/sec	Nodes	SMR	HT-MMR: 50 m/sec	HT-MMR: 100 m/sec	Nodes	SMR	HT-MMR: 50 m/sec	HT-MMR: 100 m/sec
5	16.779	15.4	13.8	5	10.51	9.56	8.76	5	672.001	722.8	711.254
10	10.704	9.89	9.6	10	7.44	7.15	6.38	10	606.004	699.2	601.29
15	7.891	7	5.98	15	5.46	4.6	4.09	15	764.662	793.951	690.527
20	7.1	6.08	6.11	20	3.38	3.15	3.09	20	735.545	649.4	688
Live Nodes											
Rounds	0	50	100	150	200	250	300	350	400	450	500
SMR	20	20	18	8	3	3	3	3	3	0	0
HT-MMR	20	20	16	8	8	8	8	8	6	2	0

3.1. Average energy consumption

It is the total energy consumption in the network divided by the count of nodes in the network. It is desirable to have a lower value of energy consumption. The lower value of energy consumption indicates that less energy resource is utilized for the transmission of packets from source to destination and hence energy efficient.

$$Average\ Energy\ Consumption = \frac{Total\ energy\ consumed\ by\ all\ nodes}{Number\ of\ nodes\ in\ network} \tag{9}$$

The graphs in Figure 10 show that AEC decreases as nodes in a network decrease in both SMR and HT-MMR methods. The speed of the mobile sink has an effect on AEC as shown in the graphs. Results show that AEC is improved with a mobile sink speed of 100 m/sec except for a network of 20 nodes. Average energy consumption is reduced by 9.66% and 16.44% for sink speeds of 50 and 100 m/sec, respectively. Result verification as illustrated in Table 4 are:
− AEC in SMR= $(16.779 + 10.704 + 7.891 + 7.1)/4 = 10.6185$
− AEC in HT-MMR: $50\ m/sec = (15.4 + 9.89 + 7 + 6.08)/4 = 9.5925$
− AEC in HT-MMR: $100\ m/sec = (13.8 + 9.6 + 5.98 + 6.11)/4 = 8.8725$
− Reduction in AEC over SMR by HT-MMR: $50\ m/sec = (10.6185 − 9.5925)/10.6185 * 100 = 9.66\%$
− Reduction in AEC over SMR by HT-MMR: $100\ m/sec = (10.6185 − 8.8725)/10.6185 * 100 = 16.44\%$
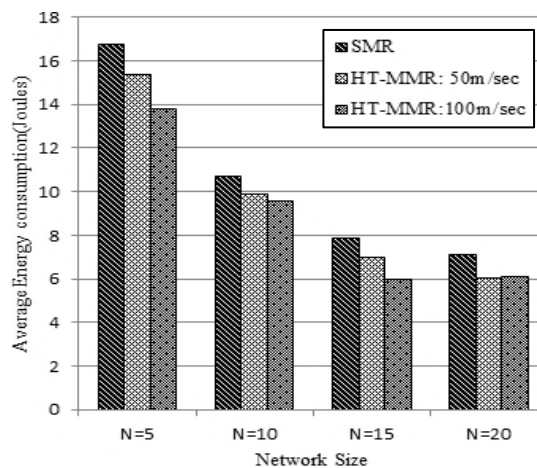

Figure 10. Average energy consumption

3.2. Energy tax

It is desirable to have a lower value for an energy tax. The higher value of energy tax indicates that more energy is spent to send a packet successfully to the destination. Energy tax is defined as the ratio of average energy consumption in the network to the count of packets received.

$$Energy\ Tax = \frac{Average\ Energy\ Consumption}{Total\ Packets\ Received} \qquad (10)$$

Experiments are conducted for two different sink speeds 50 and 100 m/sec in the HT-MMR method and results are compared with the SMR method. Energy Tax per packet decreases with an increase in nodes in both SMR and HT-MMR. HT-MMR shows a reduction in energy tax when compared to SMR. There is an improvement in energy tax when the mobile sink speed is 100 m/s rather than 50 m/s. Energy tax is reduced by 8.69% and 16.68% for sink speeds of 50 and 100 m/sec, respectively. Graphs indicating a comparative study of energy tax for SMR, and HT-MMR are shown in Figure 11. Result verification as illustrated in Table 4 are:

- AET in SMR= (10.5 + 7.44 + 5.46 + 3.38)/4 = 6.6975
- AET in HT-MMR: 50 m/sec = (9.56 + 7.15 + 4.6 + 3.15)/4 = 6.115
- AET in HT-MMR: 100 m/sec = (8.76 + 6.38 + 4.09 + 3.09)/4 = 5.58
- Reduction in AET over SMR by HT-MMR: 50 m/sec = (6.6975 − 6.115)/6.6975 ∗ 100 = 8.69%
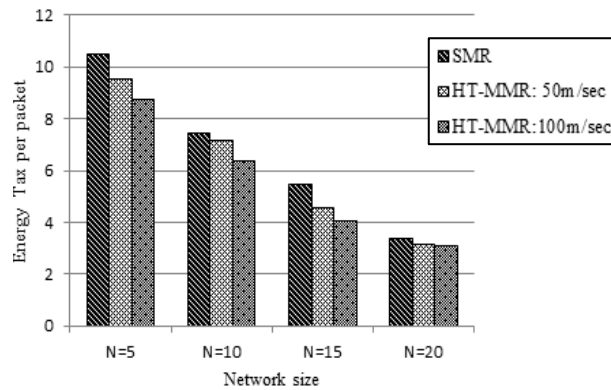- Reduction in AET over SMR by HT-MMR: 100 m/sec = 6.6975 − 5.58)/6.6975 ∗ 100 = 16.68%

Figure 11. Energy tax

3.3. Throughput

It is a measure of the success rate of packet delivery. It is desirable to have high throughput for any network. The higher the network throughput, the better the network speed. The data rate expressed in Kbps is throughput.

$$Throughput = \frac{Total\ Number\ of\ Packets\ Received ∗ Packet\ size\ in\ bytes ∗ 8}{Total\ Time} \qquad (11)$$

Simulations were carried out for SMR and HT-MMR with two different sink speeds 50 m/sec and 100 m/sec in predefined horizontal trajectories. The graphs plotted for the results obtained are shown in Figure 12. When the sink speed is 50 m/sec, the HT-MMR method shows an improvement in throughput except for a network of size 20 nodes. However, a sink speed of 100 m/sec shows an improvement in throughput only for a network of 5 nodes. Hence sink speed plays a very important role in the performance of the routing method. In our experiment 50 m/sec gives better results against the SMR method and throughput is increased by 3.14%. On the other hand, at a sink speed of 100 m/sec throughput reduces by 3.24%. Result verification as illustrated in Table 4 are:

- Throughput in SMR= (672.001 + 606.004 + 764.662 + 735.545)/4 = 694.533
- Throughput in HT-MMR: 50 m/sec = (722.8 + 699.2 + 793.951 + 649.4)/4 = 716.3377
- Throughput in HT-MMR: 100 m/sec = (711.254 + 601.29 + 690.527 + 688)/4 = 672.7677
- Improvement in throughput over SMR by HT-MMR: 50 m/sec = (716.3377 − 694.533)/694.533 ∗ 100 = 3.139%
- Improvement in throughput over HT-MMR: 100 m/sec by SMR = (694.533 − 672.7677)/672.7677 ∗ 100 = 3.24%.
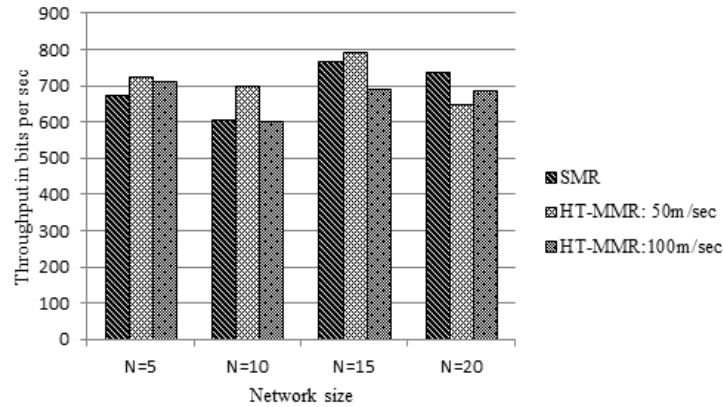
Figure 12. Throughput

3.4. Live nodes

Further simulations were carried out for 20 nodes using both SMR and HT-MMR methods (mobile sink speed=100 m/sec) by varying the number of rounds from 50 to 500 in steps of 50 rounds and the total number of live nodes is determined in each case. For simulation, only one node from each layer is generating CBR traffic for both SMR and HT-MMR scenarios. The results obtained are shown in Figure 13. From the graph, it is evident that the number of live nodes is more in HT-MMR than in SMR. In HT-MMR 40 % of nodes are alive at the end of 350 rounds and in SMR nodes alive are only 15%. Hence there is an overall 25% increase in the number of live nodes due to HT-MMR. The SMR network becomes dead for 450 rounds whereas the HT-MMR network becomes dead at the end of 500 rounds. Hence results show that HT-MMR enhances network lifetime by 11.11%. Result verification is illustrated in Table 4.

– Number of nodes alive at end of 350 rounds in $SMR = 3$
– % of nodes alive at end of 350 rounds in $SMR = 3/20 * 100 = 15$
– Number of nodes alive at end of 350 rounds in $HT - MMR = 8$
– % of nodes alive at end of 350 rounds in $HT - MMR = 8/20 * 100 = 40$
– Overall increase in live nodes $= (8 - 3)/20 * 100 = 25 \%$
– Improvement in network lifetime over SMR by $HT - MMR = (500 - 450)/450 * 100 = 11.11\%$
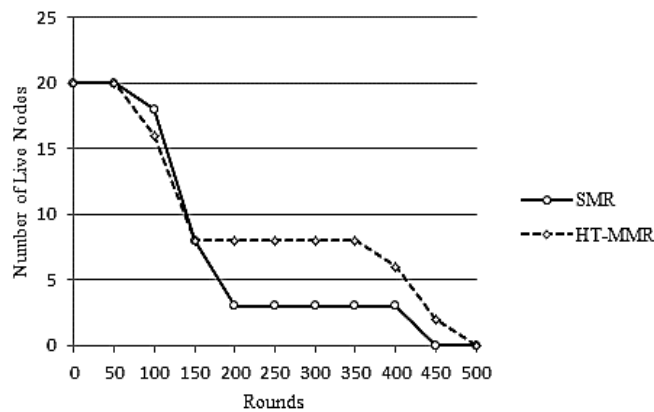

Figure 13. Network live nodes

3.5. Confidence intervals

Confidence intervals (CI) for two different confidence levels 95% and 90% are tabulated in Table 5 for energy consumption, energy tax, and throughput. CI is a range of the true mean of a population. When the population means and standard deviations are unknown CI is computed using (12).

$$Confidence\ Interval = Mean \pm Margin\ of\ Error = x \pm t * \frac{s}{\sqrt{n}} \qquad (12)$$

In (12), *x* is the sample mean, *t* is the *t*-score value at a specified confidence level, *s* is the standard deviation and *n* is the sample size. Ninety-five percent CI for energy consumption (Joules) is in the range of 3.64-17.60 (SMR), 2.91-16.27 (HT-MMR: 50 m/sec), and 3.00-14.74 (HT-MMR: 100 m/sec). 90% CI range for energy consumption (Joules) is 5.46-15.78 (SMR), 4.65-14.53 (HT-MMR: 50 m/sec), and 4.53-13.21 (HT-MMR: 100 m/sec). The *t*-score value increases with an increase in confidence level. Hence, the higher the confidence level, the higher the *t*-score value. This results in a higher margin of error. Therefore, CI increases with an increase in confidence level. At both 95% and 90% confidence levels the calculations show that CI for the population mean for energy consumption in SMR is more than in HT-MMR.

Table 5. Confidence intervals for 95% and 90% confidence levels

Performance Metrics		Energy Consumption (Joules)			Energy Tax (mjoules per packet)			Throughput (Bits per sec)		
Routing Method		SMR	HT-MMR: 50 m/sec	HT-MMR: 100 m/sec	SMR	HT-MMR: 50 m/sec	HT-MMR: 100 m/sec	SMR	HT-MMR: 50 m/sec	HT-MMR: 100 m/sec
Statistical Parameters	Average	10.6185	9.5925	8.8725	6.6975	6.1150	5.5800	694.5530	716.3378	672.7678
	Standard deviation	4.3886	4.1982	3.6882	3.0345	2.8299	2.5280	70.5812	60.1108	48.7773
				95% Confidence Level t-Value=3.182						
	Margin of Error	6.9822	6.6793	5.8679	4.8278	4.5024	4.0221	112.2948	95.6364	77.6047
	Lower_ Bound	3.6363	2.9132	3.0046	1.8697	1.6126	1.5579	582.2582	620.7014	595.1631
	Upper_ Bound	17.6007	16.2718	14.7404	8.5672	7.7276	7.1379	806.8478	811.9741	750.3724
	Confidence Interval	3.64 to 17.60	2.91 to 16.27	3.00 to 14.74	1.87 to 8.57	1.61 to 7.73	1.56 to 7.14	582.26 to 806.85	620.70 to 811.97	595.16 to 750.37
				90% Confidence Level t-Value=2.353						
	Margin of Error	5.1631	4.9392	4.3391	3.5700	3.3294	2.9742	83.0388	70.7204	57.3865
	Lower_ Bound	5.4554	4.6533	4.5334	3.1275	2.7856	2.6058	611.5142	645.6173	615.3813
	Upper_ Bound	15.7816	14.5317	13.2116	10.2675	9.4444	8.5542	777.5918	787.0582	730.1542
	Confidence Interval	5.46 to 15.78	4.65 to 14.53	4.53 to 13.21	3.13 to 10.27	2.79 to 9.44	2.06 to 8.55	611.51 to 777.59	645.62 to 787.06	615.38 to 730.15

Ninety-five percent CI for energy tax (mjoules per packet) is in the range of 1.87-8.57 (SMR), 1.61-7.73 (HT-MMR: 50 m/sec), and 1.56-7.14 (HT-MMR: 100 m/sec). 90% CI for energy tax (mjoules per packet) is in the range of 3.13-10.27 (SMR), 2.79-9.44 (HT-MMR: 50 m/sec), and 2.06-8.55 (HT-MMR: 100 m/sec). The results show that SMR has a wider CI for the true population mean of energy tax compared to HT-MMR. 95% CI for throughput (Bits per Sec) is in the range 582.26-806.85 (SMR), 620.70-811.97 (HT-MMR: 50 m/sec), and 595.16-750.37 (HT-MMR: 100 m/sec). Ninety percent CI for throughput (bits per Sec) is in the range 611.51-777.59 (SMR), 645.62-787.06 (HT-MMR: 50 m/sec), and 615.38-730.15 (HT-MMR: 100 m/sec). CI for the population means of throughput is improved for a sink speed of 50 m/sec HT-MMR in comparison with SMR. At a sink speed of 100 m/sec throughputs, the upper bound value of CI of HT-MMR is less than the upper bound value of SMR throughput. This leads to the conclusion that HT-MMR throughput is not always higher than SMR throughput.

4. CONCLUSION

In this paper, two routing methods SMR and HT-MMR have been discussed for static 3D environments. Performance evaluation of routing methods is done by determining average energy consumption, energy tax, and throughput for both methods. HT-MMR is simulated for two different mobile sink speeds: 50 m/sec and 100 m/sec. The proposed HT-MMR is energy efficient as there is a reduction in energy consumption by 16.44% and energy tax by 16.68% against the SMR method when the sink speed is 100 m/sec. There is an improvement in live nodes due to sink mobility with the horizontal trajectory in HT-MMR and the network lifetime is enhanced by 11.11%. Throughput is improved only for 50 m/sec sink speed by 3.14%. Confidence intervals for energy consumption, energy tax, and throughput are computed for 95% and 90% confidence levels. Confidence intervals for average energy consumption in Joules at 95% confidence level are 13.96 (3.64-17.60), 13.36 (2.91-16.27), 11.74 (3.00-14.74) respectively for SMR,

HT-MMR:50 m/sec, and HT-MMR: 100 m/sec. Ninety-five percent CI for energy tax (mjoules per packet) is 6.7 (1.87-8.57) for SMR, 6.12 (1.61-7.73) for HT-MMR: 50 m/sec and 5.58 (1.56-7.14) for HT-MMR: 100 m/sec. Confidence intervals for throughput in Bits per sec at 95% confidence level are 224.59 (582.26-806.85), 191.27 (620.70-811.97), 155.21 (595.16-750.37) respectively for SMR, HT-MMR: 50 m/sec and HT-MMR: 100 m/sec. These results indicate that at 100 m/sec sink speed HT-MMR has not improved throughput performance.

REFERENCES

[1] P. Xie, J.-H. Cui, and L. Lao, "VBF: vector-based forwarding protocol for underwater sensor networks," in *International conference on research in networking*, Springer Berlin Heidelberg, 2006, pp. 1216–1221.

[2] N. Nicolaou, A. See, P. Xie, J.-H. Cui, and D. Maggiorini, "Improving the robustness of location-based routing for underwater sensor networks," in *OCEANS 2007-Europe*, Jun. 2007, pp. 1–6, doi: 10.1109/OCEANSE.2007.4302470.

[3] K. M. Pouryazdanpanah, M. Anjomshoa, S. A. Salehi, A. Afroozeh, and G. M. Moshfegh, "DS-VBF: Dual sink vector-based routing protocol for underwater wireless sensor network," in *2014 IEEE 5th Control and System Graduate Research Colloquium*, Aug. 2014, pp. 227–232, doi: 10.1109/ICSGRC.2014.6908727.

[4] G. Zhang, C. Wang, L. Zhang, and Y. Shao, "Improvement research of underwater sensor network routing protocol HHVBF," in *11th International Conference on Wireless Communications, Networking and Mobile Computing (WiCOM 2015)*, 2015, doi: 10.1049/cp.2015.0744.

[5] T. Wu and N. Sun, "A reliable and evenly energy consumed routing protocol for underwater acoustic sensor networks," in *2015 IEEE 20th International Workshop on Computer Aided Modelling and Design of Communication Links and Networks (CAMAD)*, Sep. 2015, pp. 299–302, doi: 10.1109/CAMAD.2015.7390528.

[6] H. Yan, Z. J. Shi, and J.-H. Cui, "DBR: depth-based routing for underwater sensor networks," in *NETWORKING 2008 Ad Hoc and Sensor Networks, Wireless Networks, Next Generation Internet*, Springer Berlin Heidelberg, 2008, pp. 72–86.

[7] A. Wahid, S. Lee, H.-J. Jeong, and D. Kim, "EEDBR: energy-efficient depth-based routing protocol for underwater wireless sensor networks," in *Communications in Computer and Information Science*, Springer Berlin Heidelberg, 2011, pp. 223–234.

[8] N. Ilyas *et al.*, "Extended lifetime based elliptical sink-mobility in depth based routing protocol for UWSNs," in *2015 IEEE 29th International Conference on Advanced Information Networking and Applications Workshops*, Mar. 2015, pp. 297–303, doi: 10.1109/WAINA.2015.130.

[9] S. Mahmood *et al.*, "Forwarding nodes constraint based DBR (CDBR) and EEDBR (CEEDBR) in underwater WSNs," *Procedia Computer Science*, vol. 34, pp. 228–235, 2014, doi: 10.1016/j.procs.2014.07.015.

[10] H. Kaur and D. Goyal, "Link state and forwarding nodes constraint based DBR in UWSN (LCDBR)," in *2016 5th International Conference on Reliability, Infocom Technologies and Optimization (Trends and Future Directions) (ICRITO)*, Sep. 2016, pp. 277–282, doi: 10.1109/ICRITO.2016.7784965.

[11] A. Sher *et al.*, "Monitoring square and circular fields with sensors using energy-efficient cluster-based routing for underwater wireless sensor networks," *International Journal of Distributed Sensor Networks*, vol. 13, no. 7, Jul. 2017, doi: 10.1177/1550147717717189.

[12] S. Wang, T. L. N. Nguyen, and Y. Shin, "Data collection strategy for magnetic induction based monitoring in underwater sensor networks," *IEEE Access*, vol. 6, pp. 43644–43653, 2018, doi: 10.1109/ACCESS.2018.2861946.

[13] S. Wang, T. L. N. Nguyen, and Y. Shin, "Energy-efficient clustering algorithm for magnetic induction-based underwater wireless sensor networks," *IEEE Access*, vol. 7, pp. 5975–5983, 2019, doi: 10.1109/ACCESS.2018.2889910.

[14] G. Khan, K. K. Gola, and W. Ali, "Energy efficient routing algorithm for UWSN-a clustering approach," in *2015 Second International Conference on Advances in Computing and Communication Engineering*, May 2015, pp. 150–155, doi: 10.1109/ICACCE.2015.42.

[15] R. W. L. Coutinho, A. Boukerche, L. F. M. Vieira, and A. A. F. Loureiro, "EnOR: Energy balancing routing protocol for underwater sensor networks," in *2017 IEEE International Conference on Communications (ICC)*, May 2017, pp. 1–6, doi: 10.1109/ICC.2017.7996852.

[16] Z. Jin, Z. Ji, and Y. Su, "An evidence theory based opportunistic routing protocol for underwater acoustic sensor networks," *IEEE Access*, vol. 6, pp. 71038–71047, 2018, doi: 10.1109/ACCESS.2018.2881473.

[17] M. A. Rahman, Y. Lee, and I. Koo, "EECOR: An energy-efficient cooperative opportunistic routing protocol for underwater acoustic sensor networks," *IEEE Access*, vol. 5, pp. 14119–14132, 2017, doi: 10.1109/ACCESS.2017.2730233.

[18] T. Hu and Y. Fei, "QELAR: A machine-learning-based adaptive routing protocol for energy-efficient and lifetime-extended underwater sensor networks," *IEEE Transactions on Mobile Computing*, vol. 9, no. 6, pp. 796–809, Jun. 2010, doi: 10.1109/TMC.2010.28.

[19] T. Hu and Y. Fei, "An adaptive and energy-efficient routing protocol based on machine learning for underwater delay tolerant networks," in *2010 IEEE International Symposium on Modeling, Analysis and Simulation of Computer and Telecommunication Systems*, Aug. 2010, pp. 381–384, doi: 10.1109/MASCOTS.2010.45.

[20] S. Wang and Y. Shin, "Efficient routing protocol based on reinforcement learning for magnetic induction underwater sensor networks," *IEEE Access*, vol. 7, pp. 82027–82037, 2019, doi: 10.1109/ACCESS.2019.2923425.

[21] J. Chen, X. Wu, and G. Chen, "REBAR: A reliable and energy balanced routing algorithm for UWSNs," in *2008 Seventh International Conference on Grid and Cooperative Computing*, Oct. 2008, pp. 349–355, doi: 10.1109/GCC.2008.12.

[22] E. Magistretti, J. Kong, U. Lee, M. Gerla, P. Bellavista, and A. Corradi, "A mobile delay-tolerant approach to long-term energy-efficient underwater sensor networking," in *2007 IEEE Wireless Communications and Networking Conference*, 2007, pp. 2866–2871, doi: 10.1109/WCNC.2007.531.

[23] S. Gopi, K. Govindan, D. Chander, U. B. Desai, and S. N. Merchant, "E-PULRP: energy optimized path unaware layered routing protocol for underwater sensor networks," *IEEE Transactions on Wireless Communications*, vol. 9, no. 11, pp. 3391–3401, Nov. 2010, doi: 10.1109/TWC.2010.091510.090452.

[24] Z. Rahman, F. Hashim, M. Othman, and M. F. A. Rasid, "Reliable and energy efficient routing protocol (REEP) for underwater wireless sensor networks (UWSNs)," in *2015 IEEE 12th Malaysia International Conference on Communications (MICC)*, Nov. 2015, pp. 24–29, doi: 10.1109/MICC.2015.7725401.

[25] T. Ali, L. T. Jung, and S. Ameer, "Flooding control by using angle based cone for UWSNs," in *2012 International Symposium on Telecommunication Technologies*, Nov. 2012, pp. 112–117, doi: 10.1109/ISTT.2012.6481574.

[26] J. S. Abbasi *et al.*, "Balanced energy efficient rectangular routing protocol for underwater wireless sensor networks," in *2017 13th International Wireless Communications and Mobile Computing Conference (IWCMC)*, Jun. 2017, pp. 1634–1640, doi: 10.1109/IWCMC.2017.7986529.

[27] S. M. Ghoreyshi, A. Shahrabi, and T. Boutaleb, "An underwater routing protocol with void detection and bypassing capability," in *2017 IEEE 31st International Conference on Advanced Information Networking and Applications (AINA)*, Mar. 2017, pp. 530–537, doi: 10.1109/AINA.2017.82.

[28] V. R. Patil and A. Kanavalli, "Multi-sink routing protocol for underwater sensor networks," in *Information and Communication Technology for Competitive Strategies (ICTCS 2020)*, Springer Singapore, 2022, pp. 1015–1031.

BIOGRAPHIES OF AUTHORS

Vijayalaxmi R. Patil 🆔 📇 ᔆᶜ 🔾 is a research scholar at Visvesvaraya Technological University (VTU). She is currently working as an assistant professor in the Information Science and Engineering Department, Dr. Ambedkar Institute of Technology, Bangalore. She is serving the institution for the past 15 years. She is a senior member of the Computer Society of India (CSI) and a life member of the Institution of Electronics and Telecommunication Engineers (IETE). Her areas of interest include wireless sensor networks, computer networks and data communications, cryptography, and network security. She can be contacted at vijumalghan@gmail.com or vijayalaxmirp.is@drait.edu.in.

Anita Kanavalli 🆔 📇 ᔆᶜ 🔾 received her Ph.D. in Computer Science and Engineering from Bangalore University in 2013. She has published many research papers in International Conferences and Journals. She is a member of the Indian Society of Technical Education (ISTE) and IEEE (Computer Society). She has guided many MTech students and is guiding Ph.D. scholars. She is serving the institution for the past 20+ years. She is also a certified instructor for CISCO Networking Academy for CCNA. Dr. Anita Kanavalli has wide experience in teaching engineering students both at UG and PG. She has guided many projects in UG and PG. She has been actively involved in research works in the area of computer networks, sensor network applications, pervasive computing, SDN, middleware technologies, and big data. She was also a co-investigator for a project "Setting Up a Sensor Network Testbed" funded by UGC New Delhi. She can be contacted at hod_arids@msrit.edu or anithak@msrit.edu.